online data

A CBS domain-containing pyrophosphatase of *Moorella thermoacetica* is regulated by adenine nucleotides

Joonas JÄMSEN*[1], Heidi TUOMINEN*[1], Anu SALMINEN*, Georgiy A. BELOGUROV*[2], Natalia N. MAGRETOVA†, Alexander A. BAYKOV†[3] and Reijo LAHTI*[3]

*Department of Biochemistry and Food Chemistry, University of Turku, FIN-20014 Turku, Finland, and †A. N. Belozersky Institute of Physico-Chemical Biology, Moscow State University, Moscow 119899, Russia

CBS (cystathionine β-synthase) domains are found in proteins from all kingdoms of life, and point mutations in these domains are responsible for a variety of hereditary diseases in humans; however, the functions of CBS domains are not well understood. In the present study, we cloned, expressed in *Escherichia coli*, and characterized a family II PPase (inorganic pyrophosphatase) from *Moorella thermoacetica* (*mt*CBS-PPase) that has a pair of tandem 60-amino-acid CBS domains within its N-terminal domain. Because *mt*CBS-PPase is a dimer and requires transition metal ions (Co^{2+} or Mn^{2+}) for activity, it resembles common family II PPases, which lack CBS domains. The *mt*CBS-PPase, however, has lower activity than common family II PPases, is potently inhibited by ADP and AMP, and is activated up to 1.6-fold by ATP. Inhibition by AMP is competitive, whereas inhibition by ADP and activation by ATP are both of mixed types. The nucleotides are effective at nanomolar (ADP) or micromolar concentrations (AMP and ATP) and appear to compete for the same site on the enzyme. The nucleotide-binding affinities are thus 100–10000-fold higher than for other CBS-domain-containing proteins. Interestingly, genes encoding CBS-PPase occur most frequently in bacteria that have a membrane-bound H^+-translocating PPase with a comparable PP_i-hydrolysing activity. Our results suggest that soluble nucleotide-regulated PPases act as amplifiers of metabolism in bacteria by enhancing or suppressing ATP production and biosynthetic reactions at high and low [ATP]/([AMP] + [ADP]) ratios respectively.

Key words: adenine nucleotide, bidirectional regulation, cystathionine β-synthetase domain (CBS domain), inorganic pyrophosphatase (PPase), *Moorella thermoacetica*.

INTRODUCTION

PP_i (inorganic pyrophosphate) is produced in vast amounts by biosynthetic reactions, such as protein, RNA and DNA synthesis, and its concentration affects the equilibria of these reactions [1]. In addition, PP_i regulates many other cellular processes, including calcification, cell proliferation and iron transport [2]. Consequently, disruption of PP_i metabolism can lead to a variety of pathological conditions [2].

PP_i is mainly hydrolysed to P_i (orthophosphate) by PPase (inorganic pyrophosphatase) (EC 3.6.1.1), an enzyme that is essential for life [3–6]. There are two known types of PPase: soluble and integral membrane-bound. Soluble PPases are subdivided further into families I and II, which are not homologous [7,8]. Family I PPases are found in all kingdoms of life and are among the best-characterized phosphoryl transfer enzymes [9,10]. Family II PPases, which were discovered more recently [7,8], are found in Bacilli and Clostridia and in some other bacterial lineages, including several human pathogens, and belong to the DHH (Asp-His-His) family of phosphohydrolases [11]. Family II PPases are homodimers of subunits formed by two well-defined domains, whereas family I PPases have two or six compact one-domain subunits. The N- and C-terminal domains of family II PPases are connected by a flexible linker, and the active site is located at the domain interface [12,13]. Also, unlike family I PPases, family II PPases contain a tightly bound transition metal ion, usually Mn^{2+} or Co^{2+}, although they also require Mg^{2+} for maximal activity. In addition, bivalent cations, especially Mn^{2+}, promote dimerization of family II PPases [14].

Interestingly, the N-terminal domain of approx. 25 % of the known family II PPase sequences contains a large (~250-amino-acid) insert, comprising two CBS (cystathionine β-synthase) domains. None of these CBS-PPases has been isolated and characterized. CBS domains, originally found in cystathionine β-synthase [15], are widely distributed among proteins in all three kingdoms of life, but their roles are not well understood [16,17]. In some cases, CBS domains are potential targets for regulation by adenosine derivatives [16–21]. Importantly, point mutations in CBS domains cause several hereditary diseases in humans [17].

To elucidate the role of CBS domains in family II PPases, we have cloned, expressed and purified a CBS-PPase from *Moorella thermoacetica* (formerly known as *Clostridium thermaceticum*) (*mt*CBS-PPase), a low-G + C Gram-positive thermophilic acetogen with an optimum growth temperature of 55–60 °C [22]. We found that, unlike all other known PPases, this enzyme is subject to a strong bidirectional regulation by adenine nucleotides.

EXPERIMENTAL

Cloning and mutagenesis

Genomic DNA extracted from *M. thermoacetica* strain ATCC 35608 was obtained from DSMZ (Deutsche Sammlung von

Abbreviations used: CBS, cystathionine β-synthase; DTPA, diethylenetriaminepenta-acetic acid; PPase, inorganic pyrophosphatase; *mt*CBS-PPase, CBS domain-containing PPase from *Moorella thermoacetica*.

[1] These authors contributed equally to this work.

[2] Present address: Department of Microbiology and The RNA Group, The Ohio State University, 484 West 12th Avenue, Columbus, OH 43210, U.S.A.

[3] Correspondence may be addressed to either of these authors (email baykov@genebee.msu.su or reijo.lahti@utu.fi).

Mikroorganismen und Zellkulturen GmbH). The *mt*CBS-PPase open reading frame (GenBank® accession number NC_007644) was amplified by PCR using primers 5′-TTATC-ATATGGGTAAAGAGATTCTGGTTATCG-3′ (forward) and 5′-TTATCTCGAGTTATCCCTGCAGCAACCGCCG-3′ (reverse). The amplified gene was sequenced in both directions, and one difference compared with the sequence shown in GenBank® was observed (TTG encoding Leu^{190} was replaced by CTG), but this did not affect the protein sequence. The PCR fragment was inserted via the pET36b vector (Novagen) into pBluescript SK (Stratagene), and site-directed mutagenesis was performed using an overlapping PCR technique (QuikChange®, Stratagene). The mutation was verified by DNA sequencing.

Protein expression and purification

To produce wild-type and variant *mt*CBS-PPases, the PCR products were cloned into the pET36b vector using NdeI and XhoI. The plasmid construct was transformed into *Escherichia coli* BL21(DE3) RIL cells (Stratagene), and the transformants were grown in Terrific broth [23] containing 30 μg/ml kanamycin and 30 μg/ml chloramphenicol. *mt*CBS-PPase expression was induced for 3 h using 0.4 mM IPTG (isopropyl β-D-thiogalactoside).

Cell paste (10 g wet weight) obtained by centrifugation at 6300 ***g*** for 10 min was resuspended in 30 ml of ice-cold 25 mM Tris/HCl buffer (pH 7.3), containing 24 mM $MgCl_2$, 1 mM $CoCl_2$, 20 μM DTPA (diethylenetriaminepenta-acetic acid), and was homogenized twice using a French press (SLM Instruments) at 900 p.s.i. (1 p.s.i. = 6.9 kPa). The crude extract obtained was loaded on to a 150 ml column containing Fast Flow DEAE-Sepharose (GE Healthcare). The column was washed with the same buffer, and protein was eluted with a 450 ml linear gradient of 0.1–0.3 M NaCl. Fractions containing *mt*CBS-PPase (150–190 mM NaCl) were pooled, concentrated to 12 ml with Centriprep 10 (Amicon), and purified further by gel filtration on a Superdex 200 26/60 column (GE Healthcare) equilibrated with 50 mM Tris/HCl buffer (pH 7.5), containing 50 mM KCl, 2 mM $MgCl_2$, 0.1 mM $CoCl_2$ and 20 μM DTPA. The fractions containing *mt*CBS-PPase were pooled, concentrated to 20–40 mg/ml and were stored frozen at −70 °C.

Because the enzyme was most stable in the presence of 0.1 mM Co^{2+} and 2 mM Mg^{2+}, these cations were routinely added to the solutions used to purify, store and dilute the enzyme. When needed, these metal ions were removed from the enzyme stocks by incubation with 5 mM DTPA for 1 day at 4 °C. The bulk of the chelator was removed by dialysis against three 1 litre changes of 100 mM Mops/KOH buffer (pH 7.5) containing 50 μM DTPA.

The purity of enzyme samples was assessed by electrophoresis on 8–25 % gradient polyacrylamide gels in the presence of 0.55 % SDS using the Phast System (GE Healthcare). Concentrations of *mt*CBS-PPase solutions were determined on the basis of a subunit molecular mass of 48.1 kDa and a specific absorption coefficient $A_{280}^{1\%}$ of 4.5, as estimated from the amino acid composition using the ProtParam program [24].

Activity measurements

Except where noted, the activity was measured at 25 °C in 25 ml of 100 mM Mops/KOH buffer (pH 7.2) containing 0.1 mM $CoCl_2$, 5 mM $MgCl_2$ and the nucleotide tested. An aliquot (5–150 μl) of diluted enzyme solution was added to the mixture (0.2–2 μg/ml final enzyme concentration), followed 1 min later by 0.16 mM PP_i. The formation of P_i was then monitored for 3–10 min using an automatic P_i analyser [25], and initial reaction rates were estimated from the recorder tracing.

AMP, ADP and ATP were from Fluka. All other nucleotides were from Sigma. AMP was the free acid, ADP was the potassium salt, and all other nucleotides were sodium salts. Immediately before the use of ATP, any contaminating ADP was converted into ATP by treating 5 mM stock solutions of ATP for 1 h at room temperature (23 ± 2 °C) with 10 units/ml rabbit muscle creatine kinase (Roche) in 100 mM Mops/KOH buffer (pH 7.2) containing 10 mM phosphocreatine (Fluka) and 5 mM $MgCl_2$. The AMP preparation was judged to be reasonably pure because a similar treatment with creatine kinase and phosphocreatine had no effect on the PPase activity measured in the presence of AMP. In addition, treating stock ADP solutions with 10 units/ml hexokinase and 10 mM glucose to convert any contaminating ATP into ADP also had no effect on the PPase activity. For competition measurements, in which ADP and ATP were added simultaneously, creatine kinase in stock solutions of ATP was removed by ultrafiltration using 4 ml Vivaspin concentrators (Sartorius AG) with a 10 kDa molecular-mass cut-off PES (polyethersulfone) membrane.

Sedimentation

Analytical ultracentrifugation was carried out at 20 °C in a Spinco E instrument (Beckman Instruments) with scanning at 280 nm. The samples contained 10 μM enzyme and appropriate ligands. Before each run, the samples were incubated for 2–3 h at 20 °C. The sedimentation velocity was measured at 48 000 rev./min, and the sedimentation coefficient ($s^0_{20,w}$) was calculated as described by Chervenka [26].

Cross-linking and electrophoresis

Enzyme was diluted to 8.3 μM with 25 mM Hepes/KOH (pH 7.5) and then incubated with 26 mM glutaraldehyde for 15 or 30 min at room temperature [27]. The reaction was stopped by addition of 1/10 vol. of 1.0 M Tris/HCl (pH 7.3). The samples were separated by electrophoresis on Phast System SDS/8–25 % PAGE gradient gels (GE Healthcare), and the gels were stained with PhastGel Blue R (GE Healthcare). A Perfect Protein Marker kit (Novagen) was used for molecular-mass standards.

Kinetic data analysis

Non-linear least squares fitting of the data was performed using SCIENTIST, version 2.01 (Micromath). The dependence of activity on the concentration of the ligand (L) was fitted to eqn (1), where A_{+L} and A_{-L} are activities with and without bound ligand respectively, and K_d is the apparent dissociation constant of the enzyme–ligand complex, all measured at a fixed substrate concentration:

$$A = A_{+L} + (A_{-L} - A_{+L})/(1 + [L]/K_d) \quad (1)$$

In competition experiments, the dependence of the apparent K_d ($K_{d,app}$) for ligand L_1 on the concentration of the second ligand, L_2, was fitted to eqn (2), where K_{d1} and K_{d2} are the dissociation constants for ligands L_1 and L_2 respectively:

$$K_{d,app} = K_{d1}(1 + [L_2]/K_{d2}) \quad (2)$$

RESULTS

Expression, purification and catalytic activity of *mt*CBS-PPase

SDS/PAGE analysis of crude extracts obtained from recombinant *E. coli* cells revealed an intense ~50 kDa band that was absent in cells transformed with empty pET36b vector (results not shown).

Table 1 Effects of nucleotides and nucleosides (100 μM) on Co^{2+}/Mg^{2+}-activated *mt*CBS-PPase

The activity of *mt*CBS-PPase measured with no effector added (1.64 s^{-1}) was taken as 100 %.

Effector	Activity (%)
None	100
Adenosine	94 ± 2
AMP	4.0 ± 0.1
ADP	< 1
ATP	158 ± 2
cAMP	42 ± 4
CDP	50 ± 8
GMP	82 ± 3
GDP	81 ± 3
UDP	65 ± 8
UTP	96 ± 2
Cytidine, guanosine, uridine, CMP, CTP, GTP, cGMP, UMP	100 ± 3

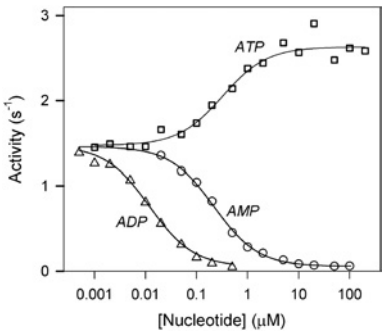

Figure 1 Effects of adenine nucleotides on Co^{2+}/Mg^{2+}-activated *mt*CBS-PPase

The lines show the best fit to eqn (1).

The SDS/PAGE also indicated that *mt*CBS-PPase represented ~10 % of the total protein. The recombinant protein was easily purified to homogeneity by ion-exchange chromatography and gel filtration. This procedure yielded 30–40 mg of pure *mt*CBS-PPase per litre of cell culture (~6 g of cell paste). *E. coli* PPase, which belongs to family I of soluble PPases, was absent from the purified *mt*CBS-PPase, because the former was eluted at a 20 mM lower NaCl concentration during DEAE-Sepharose chromatography.

The purified *mt*CBS-PPase exhibited a maximal k_{cat} value (1.7 s^{-1}) when assayed in the presence of both 1 mM Mg^{2+} and 0.1 mM Co^{2+}. Replacement of Co^{2+} by Mn^{2+} decreased k_{cat} to 0.65 s^{-1}. The k_{cat} values observed in the presence of Co^{2+}, Mn^{2+} or Mg^{2+} alone were 1.15, 0.36 and 0.01 s^{-1} respectively. According to its cofactor specificity, *mt*CBS-PPase resembles the common family II PPase of *Methanococcus jannaschii* [28]. However, the maximal observed k_{cat} value for *mt*CBS-PPase at 25 °C was three orders of magnitude lower than that for common family II PPases [14] and was only 2-fold higher at 55 °C, the growth temperature of *M. thermoacetica*.

Effects of nucleotides and nucleosides

Table 1 shows that *mt*CBS-PPase is strongly inhibited by 100 μM AMP and ADP, whereas ATP activates it 1.6-fold. Some nucleotides, including cAMP, CDP and UDP were less effective at inhibiting *mt*CBS-PPase, and most other nucleotides and nucleosides did not significantly affect the activity. Thus adenine nucleotides are effective modulators of *mt*CBS-PPase activity. This is strikingly different from the common family II PPase from *Bacillus subtilis* and family I PPases from *E. coli* and other sources, which are not modulated by ATP, ADP or AMP and lack CBS domains.

Kinetic analysis of adenine nucleotide effects

Figure 1 shows the dose-dependencies of AMP, ADP and ATP effects measured at a fixed substrate concentration (160 μM total PP_i). Each curve obeyed eqn (1) for activation or non-linear inhibition with a finite activity of the enzyme–inhibitor complex. The relative values of these activities (A_{+L}/A_{-L}) for AMP and ADP were low, but significantly different from zero (Table 2). The apparent binding constants (K_d) derived for each nucleotide from these profiles are also summarized in Table 2. As expected from the appearance of the profiles in Figure 1, the K_d values were similar for AMP and ATP, and an order of magnitude lower for ADP.

The nucleotide effects on activity were analysed further using a Lineweaver–Burk plot. Surprisingly, the inhibition by AMP and ADP was of different types. AMP increased only the Michaelis constant (Figure 2, upper panel) and was thus a competitive inhibitor, whereas ADP additionally decreased the maximal velocity (Figure 2, lower panel) and was thus a mixed-type inhibitor. The effect of ATP on the kinetic parameters was the opposite of that of ADP (Figure 2, upper panel). At 10 μM, ATP decreased the Michaelis constant (from 10.6 ± 0.5 to 7.0 ± 0.6 μM) and increased the maximal velocity (from

Table 2 Parameters describing the effects of nucleotides on Co^{2+}- and Mn^{2+}-bound *mt*CBS-PPase

		Co^{2+}/Mg^{2+}-activated enzyme		Mn^{2+}/Mg^{2+}-activated enzyme		
Enzyme	Nucleotide	A_{+L}/A_{-L} (%)	K_d (μM)	A_{+L}/A_{-L} (%)	K_d (μM)	Source
Wild-type	AMP	3.7 ± 0.4	0.22 ± 0.02	20 ± 4	1.4 ± 0.2	Inhibition of activity (Figure 1)
	AMP	0.17 ± 0.05				Effect on ATP activation
	ADP	0.8 ± 0.3	0.012 ± 0.001	21 ± 2	0.033 ± 0.004	Inhibition of activity (Figure 1)
	ADP	0.017 ± 0.005				Effect on ATP activation (Figure 3)
	ATP	180 ± 10	0.20 ± 0.05	400 ± 40	7.2 ± 0.8	Inhibition of activity (Figure 1)
	ATP	0.16 ± 0.01				Effect on AMP inhibition
	ATP	0.6 ± 0.2				Effect on ADP inhibition (Figure 3)
	CDP	< 10	150 ± 20			Inhibition of activity
	UDP	< 10	340 ± 90			Inhibition of activity
Y169A	AMP	52 ± 2	5.3 ± 0.9			Inhibition of activity
	ADP	6.7 ± 0.4	0.21 ± 0.02			Inhibition of activity
	ATP	143 ± 4	2.4 ± 0.9			Inhibition of activity

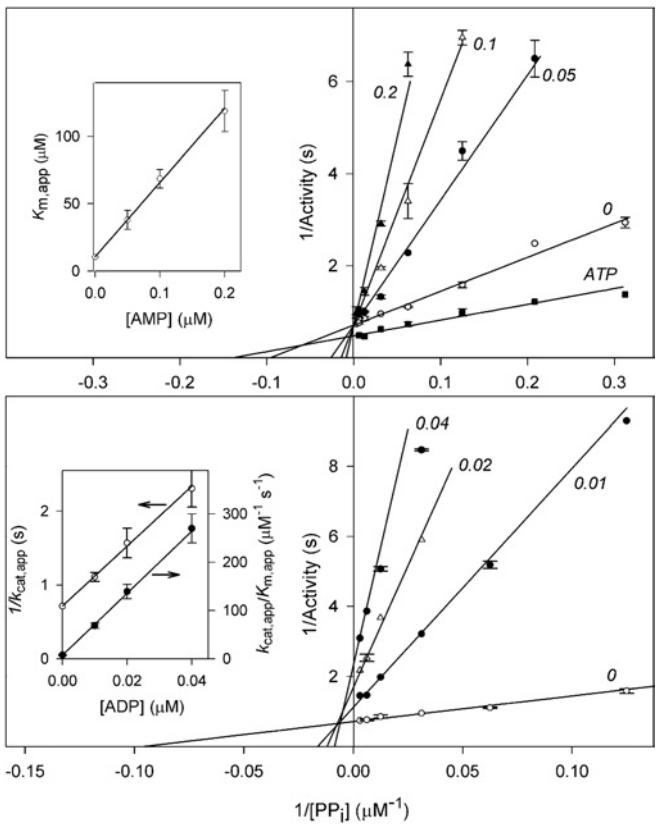

Figure 2 Lineweaver–Burk plots for *mt*CBS-PPase inhibition and activation by adenine nucleotides

Upper panel: inhibition by AMP and activation by ATP. Numbers on the lines indicate AMP concentrations (in μM). The line marked ATP shows the effect of 10 μM ATP. Lower panel: inhibition by ADP. Numbers on the lines indicate ADP concentrations (in μM). The insets show the dependencies of $K_{m,app}$ (upper panel) or $1/k_{cat,app}$ and $k_{cat,app}/K_{m,app}$ (lower panel) on nucleotide concentration.

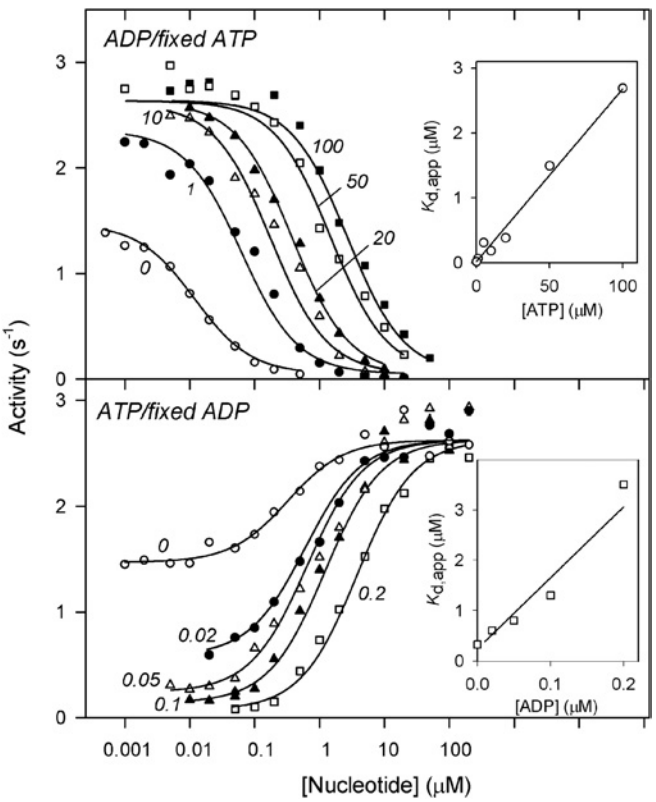

Figure 3 Combined effects of ADP and ATP on the activity of *mt*CBS-PPase

Upper panel: effect of various concentrations of ADP at several fixed concentrations of ATP. Lower panel: effect of various concentrations of ATP at several fixed concentrations of ADP. The numbers on the curves denote the fixed concentration of the second nucleotide in μM. The lines show the best fit to eqn (1). The insets show the dependences of $K_{d,app}$ on the concentration of the corresponding fixed ligand. The lines in the insets show the best fit to eqn (2).

1.69 ± 0.05 to 2.3 ± 3 s^{-1}). True inhibition constants governing AMP binding to substrate-free enzyme ($K_i = 19 \pm 2$ nM) and ADP binding to substrate-free enzyme ($K_i = 1.3 \pm 0.1$ nM), and to the enzyme–substrate complex (K_i'=0.35 ± 0.03 μM), were estimated from the secondary dependencies shown in the insets of Figure 2. The substrate thus afforded partial protection against inhibition by ADP and completely prevented inhibition by AMP. The residual activity of the nucleotide-bound enzyme was ignored in this analysis, as this activity would have only a minor effect on estimated parameter values. For ATP, true binding constants governing binding to substrate-free enzyme (K_a) and to enzyme–substrate complex (K_a') were not determined separately, but their ratio, K_a'/K_a, should be close to the ratio of the Michaelis constants measured at ATP concentrations of zero and near-saturating (10 μM), i.e. 1.5 ± 0.2. That K_a'/K_a exceeds unity is also evident by the fact that the lines measured in the absence and in the presence of ATP intersected above the x-axis in Figure 2 (upper panel).

To investigate interactions of inhibiting and activating nucleotides on *mt*CBS-PPase activity, the profiles of ADP modulation were measured at several fixed ATP concentrations and vice versa (Figure 3). ATP protected *mt*CBS-PPase from inhibition by ADP by decreasing the sensitivity to ADP (i.e. by shifting the dose–response inhibition curve to the right) and by increasing the basal activity in the absence of ADP. The $K_{d,app}$ for ADP changed in proportion to the ATP concentration (Figure 3, upper panel inset) up to 100 μM ATP, which is 500 times the K_d for ATP. Similarly, the $K_{d,app}$ for ATP was a linear function of the ADP concentration up to 0.2 μM ADP (Figure 3, lower panel inset), which is 80 times the K_d for ADP. These results indicate that the binding of ADP and ATP was mutually exclusive in the concentration ranges tested. If a mixed enzyme–ADP/ATP and/or enzyme–substrate–ADP/ATP complex was formed, $K_{d,app}$ for ADP would have attained a constant level, intermediate between the K_d values for ADP binding to enzyme–ATP and enzyme–substrate–ATP. These considerations also apply to the lower panel of Figure 3. Qualitatively similar inhibition/activation patterns were observed for the AMP/ATP pair (results not shown). The effective concentrations of AMP were, however, higher than those of ADP by an order of magnitude. The binding constants derived for each nucleotide, from results shown in the insets to Figure 3, are summarized in Table 2.

The effects of the adenine nucleotides on Mn^{2+}/Mg^{2+}-activated *mt*CBS-PPase were qualitatively similar to those observed for the Co^{2+}/Mg^{2+}-activated form (Figure 1). The K_d values for AMP and ADP were also similar, but the K_d value for ATP was 10-fold higher (Table 2). Furthermore, the relative residual activities at infinite AMP or ADP concentrations (A_{+L}/A_{-L}) were markedly higher in the presence of Mn^{2+}. Finally, AMP, ADP and ATP had similar effects on Co^{2+}/Mg^{2+}-activated *mt*CBS-PPase at 55 °C, which is the physiological temperature for *M. thermoacetica* (results not shown).

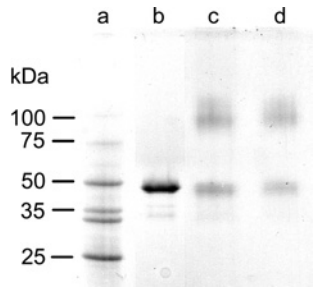

Figure 4 SDS/PAGE analysis of *mt*CBS-PPase

Lane a, molecular-mass markers; lane b, intact enzyme; lane c, enzyme cross-linked with glutaraldehyde for 15 min; lane d, enzyme cross-linked with glutaraldehyde for 30 min. Protein load for lanes b–d was 1 μg/lane.

Effect of Y169A substitution on adenine nucleotide binding

Tyr-169 is located in the CBS domain of *mt*CBS-PPase, in the region corresponding to the nucleotide-binding pocket of the chloride transporter ClC-5, another CBS domain protein whose three-dimensional structure has been determined recently [29]. Consistent with this localization, the replacement of Tyr-169 with alanine markedly decreased the affinity of *mt*CBS-PPase for the adenine nucleotides (Table 2), while having only a small effect (1.8-fold activation) on enzyme hydrolytic activity measured in their absence. Qualitatively, the Y169A variant behaved similarly to wild-type *mt*CBS-PPase and exhibited activation by ATP and inhibition by AMP and ADP (Table 2).

Quaternary structure of *mt*CBS-PPase

Common family II PPases are dimeric proteins in the presence of metal cofactors, but dissociate into nearly inactive monomers in the absence of such cofactors [14,30]. As CBS domains are reported to control oligomerization of CBS [31,32], we determined the oligomeric structure of *mt*CBS-PPase in the absence and presence of adenine nucleotides and compared it with that of common family II PPases. The sedimentation coefficient ($s^0_{20,w}$) at pH 7.2 was 6.4 ± 0.1 S for the metal-depleted *mt*CBS-PPase and increased to 7.7 ± 0.1, 7.9 ± 0.2 and 7.6 ± 0.1 S in the presence of 100 μM $CoCl_2$, 100 μM $MnCl_2$, or 1 mM $MgCl_2$ respectively. Adenine nucleotides (AMP, ADP and ATP) at 100 μM had no effect on the $s^0_{20,w}$ value for *mt*CBS-PPase measured in the presence of 100 μM $CoCl_2$.

The values of $s^0_{20,w}$ for *mt*CBS-PPase measured in the presence of the metal ions were somewhat higher than that predicted assuming a spherical protein with a molecular mass of 96 kDa (dimer of 48 kDa monomers). Therefore we performed cross-linking experiments to confirm that this enzyme is a dimer. Specifically, we reacted *mt*CBS-PPase with glutaraldehyde and separated the products by SDS/PAGE. Almost all of the protein migrated as the cross-linked dimer, although a small amount of unreacted monomer was observed (Figure 4). Similar electrophoresis patterns were obtained for *mt*CBS-PPase treated with glutaraldehyde in the presence of different metal ions or at various concentrations of *mt*CBS-PPase. The relative amount of the monomer, however, increased slightly in the absence of the metal ions or at low enzyme concentrations. Collectively, our results indicate that the oligomeric structure of *mt*CBS-PPase is similar to that of common family II PPases, which lack CBS domains, and is not affected by nucleotide binding.

DISCUSSION

CBS domains are found in both cytosolic enzymes and membrane-associated enzymes and channels from all species. They usually occur as tandem repeats, which are independent units that retain their structure and binding properties even when separated from the bulk protein [17]. The importance of CBS domains is emphasized by the observations that mutations of their conserved residues impair AMP, ATP and *S*-adenosylmethionine binding to the CBS domains and cause a variety of human hereditary diseases [16,17]. Although they are thought to be regulatory domains, the experimental evidence for this is scarce. Because CBS domains bind adenine nucleotides with varying affinities, they may act as sensors of cellular energy status [16,17]. More recently, CBS domains of the chloride channel ClC-5 have been implicated in the control of intracellular trafficking [33] and the gating of the osmoregulatory transporter OpuA by osmotic strength [34].

CBS domains as regulators of *mt*CBS-PPase

Several lines of evidence suggest that the modulation of *mt*CBS-PPase by nucleotides is also mediated by CBS domains. First, isolated CBS domains from several proteins can bind adenine nucleotides [16,17,20], whereas common family II PPases that lack CBS domains do not bind adenine nucleotides [35]. Secondly, a single Y169A replacement in the CBS domain suppressed nucleotide binding to *mt*CBS-PPase, but increased enzyme catalytic activity. Finally, the mixed-type inhibition of *mt*CBS-PPase by ADP, and the activation by ATP, indicate formation of a ternary enzyme–substrate–nucleotide complex and are therefore inconsistent with nucleotide binding at the active site.

The observed competition between ATP binding and the binding of both AMP and ADP, as well as the structural similarities between these compounds, imply a common binding site for all nucleotides on *mt*CBS-PPase. This conclusion is supported by structural data reported for other proteins. To date, a high-resolution three-dimensional structure is available only for a single intact CBS domain-containing protein, namely IMP dehydrogenase, but it does not contain bound nucleotides in the CBS domain [36]. However, three-dimensional structures have been determined for several truncated CBS domain-containing proteins [29,37,38]. The most recent structures of the cytoplasmic part of the chloride transporter ClC-5 [29] contain bound ADP or ATP, and those of the C-terminal domain of AMP-activated protein kinase (Protein Data Bank codes 2OOX and 2OOY) contain bound AMP or ATP, at the same site, formed between two CBS domains. Importantly, the new structures suggest that the nucleotides cause a marked conformational change in the CBS domains, thus explaining nucleotide regulatory action.

Although all polar active-site residues found in common family II PPases [12,13] are conserved in *mt*CBS-PPase, even in the presence of the best metal cofactor, Co^{2+}, *mt*CBS-PPase is less active than common family II PPases by three orders of magnitude. Therefore the insert containing two CBS domains appears to severely disrupt the normal catalytic cycle. Importantly, such an 'internally inhibited' system should be very sensitive to structural changes caused by nucleotide binding to the CBS domains and could easily be inhibited or activated. In this context, ATP partially compensates for the effect of the CBS insertion, whereas AMP and ADP increase the effect.

Nucleotide specificity of *mt*CBS-PPase

Nucleotide binding to *mt*CBS-PPase was highly specific with respect to both the base and the phosphate moieties. At a concentration of 100 μM, adenine nucleotides were the most

potent regulators of the enzyme. When guanine and uridine nucleotides were examined, only the diphosphates had significant effects on the activity of *mt*CBS-PPase; this may be because these nucleotides bound with weaker affinities.

The phosphate moiety of the nucleotide is also important and determines both binding affinity (adenosine does not bind) and whether the nucleotide acts as an activator or inhibitor. A diphosphate seems to result in the highest binding affinity, but a triphosphate is needed for activation. Moreover, the phosphate moiety determines the relative affinities of the nucleotide for free enzyme and the enzyme–substrate complex. AMP, ADP and ATP can all combine with substrate-free enzyme, whereas only ADP and ATP can bind, although with lower affinity, to the enzyme–substrate complex. Accordingly, the inhibition type is competitive with AMP and mixed with ADP, and ATP is a mixed-type activator. Substrate thus interferes with adenine nucleotide binding and vice versa, and the effect decreases with increases in phosphate chain length, especially when comparing AMP effects with ADP effects. A likely structural explanation of these data is that both the α-phosphate and the β-phosphate are involved in strong, thermodynamically favourable, interactions that stabilize inactive conformations of *mt*CBS-PPase, whereas the interaction with the γ-phosphate is thermodynamically unfavourable, but gives rise to an active enzyme conformation. The conformations elicited by AMP and ADP are different because their complexes bind substrate differently. Although a direct contact of the nucleotide phosphate chain with the active site cannot presently be excluded, it seems unlikely, because ATP, which has the longest phosphate chain, facilitated substrate binding by lowering K_m (Figure 2). The assumed conformational flexibility of *mt*CBS-PPase is consistent with the known structures of common family II PPases, in which active sites lie between two domains connected by a highly flexible linker [12,13]. The dependence of the nucleotide effect on the length of the phosphate moiety may be due, but only in part, to Mg^{2+} binding; in the presence of 5 mM Mg^{2+}, ATP and ADP predominantly exist as complexes with Mg^{2+}, whereas AMP exists as a mixture of free and Mg^{2+}-bound forms [39].

The effects of the adenine nucleotides vary in different CBS domain proteins. With the exception of the chloride channel ClC-1, which is inhibited by both AMP and ATP, generally AMP and ATP have opposite effects on these proteins [20]. For example, AMP activates and ATP inhibits AMP-activated protein kinase and the chloride channel ClC-2 [16,19], and, as in the case of *mt*CBS-PPase, ATP activates and AMP inhibits IMP dehydrogenase-2 and the chloride channel ClC-5. These findings have led to the hypothesis that CBS domains act as energy-sensing modules in proteins [16]. Generally, AMP, ADP and ATP bind with similar affinities to these proteins, in contrast with adenine nucleotide interactions with *mt*CBS-PPase, where ADP binding is strongly preferred. Furthermore, AMP and ATP bind at least 100-fold, and ADP 10000-fold, more tightly (in terms of K_d) to *mt*CBS-PPase than to ClC-5 [29], or to other CBS domain proteins [16].

Distribution, phylogeny and possible role of CBS-PPases

Common family II PPases predominate in Bacilli, whereas CBS-PPases predominate in Clostridia and sulfate-reducing δ-proteobacteria (see Supplementary Figure S1 at http://www.BiochemJ.org/bj/408/bj4080327add.htm). Both types of family II PPases occur sporadically in other bacterial lineages. In contrast, structurally distinct family I PPases are more widespread and occur in most of the bacterial phyla as well as in archaea and eukaryotes. Interestingly, a majority of the CBS-PPases contain an $\sim$120-amino-acid DRTGG domain [40] between two CBS domains. The function of DRTGG domains is unknown, and they are found exclusively in bacterial and archaeal proteins. CBS-PPases from *M. thermoacetica* and *Syntrophomonas wolfei* are unique in that they possess CBS domains, but lack a DRTGG domain.

Phylogenetic analysis of family II PPases suggests that all CBS-PPases are closely related, but do not form a monophyletic group (Supplementary Figure S1). Some groups of common family II PPases, notably Bacilli PPases, have probably arisen due to the secondary loss of the CBS and DRTGG domain insertion. In addition, *M. thermoacetica* and *S. wolfei* are two independent cases where the DRTGG domain appears to have been lost. Finally, the clustering of CBS-PPases near the centre of the tree suggests that the insertion was acquired very early in the evolution of family II PPases.

CBS-PPases are found in 16 of the 329 prokaryotic species with complete genome sequences in the Kyoto Encyclopedia of Genes and Genomes (http://www.genome.jp/kegg/catalog/org_list.html). Thirteen of these 16 species also have a gene encoding a membrane-bound H^+-translocating PPase (H^+-PPase). Interestingly, none of the 83 prokaryotic species with a gene for H^+-PPase has a gene for the common family II PPase. H^+-PPase may be unnecessary when there are family II PPases because the latter are three orders of magnitude more active and would therefore deplete the cell of PP_i, which H^+-PPase uses to establish a transmembrane pH gradient. In contrast, the activities of CBS-PPase and membrane-bound-PPase in *M. thermoacetica* are similar (A. Malinen, personal communication), permitting control of the PP_i concentration by the levels of adenine nucleotides via *mt*CBS-PPase.

Biosynthetic reactions are the major source of PP_i. Accordingly, in *M. thermoacetica*, the intracellular level of PP_i peaks sharply during the mid-exponential phase of growth [41]. To avoid inhibition of biosynthetic enzymes and to provide P_i for ATP synthesis, this PP_i must be efficiently degraded by PPase. In fact, during the mid-exponential phase, *mt*CBS-PPase is expected to be most active because of a high [ATP]/([ADP] + [AMP]) ratio. Interestingly, Co^{2+}, the best cofactor for *mt*CBS-PPase, is required for the growth of *M. thermoacetica* [22,42]. Metabolic stresses that decrease ATP production inhibit biosynthetic reactions and cell growth by decreasing the [ATP]/([ADP] + [AMP]) ratio. This, in turn, should inhibit *mt*CBS-PPase and allow accumulation of PP_i, which would further inhibit biosynthetic reactions. Instead of or in conjunction with the action of H^+-ATPase, the accumulated PP_i is apparently used by H^+-PPase to sustain the pH gradient across the cell membrane and therefore maintain cell vitality. This two-PPase system may allow the cell to combat stress more efficiently than cells with only soluble or membrane-bound PPases. Thus CBS-PPase may act as a survival factor under conditions of low energy supply.

In summary, unlike other PPases, *mt*CBS-PPase is subject to strong inhibition by AMP and ADP as well as activation by ATP. Remarkably, this enzyme binds adenine nucleotides much more tightly than other reported CBS proteins. Furthermore, an effect of ADP, which is the most efficient inhibitor of *mt*CBS-PPase, is uncommon in other CBS proteins. Further studies, including determination of the three-dimensional structure of *mt*CBS-PPase with a bound adenine nucleotide, are needed to elucidate the structural basis for nucleotide regulation of this interesting enzyme and other CBS proteins.

This work was supported by Academy of Finland Grants 201611 and 114706, a grant for the National Graduate School in Informational and Structural Biology from the Ministry of Education and the Academy of Finland, and Russian Foundation for Basic Research

Grant 06-04-48887. We thank University of Oslo Bioportal for providing CPU (central processing unit) time and P.V. Kalmykov (A.N. Belozersky Institute of Physico-Chemical Biology) for his assistance with analytical centrifugation.

REFERENCES

1 Kornberg, A. (1962) On the metabolic significance of phosphorolytic and pyrophosphorolytic reactions. In Horizons in Biochemistry (Kasha, M. and Pullman, B., eds.), pp. 251–264, Academic Press, New York
2 Heinonen, J. (2001) Biological Role of Inorganic Pyrophosphate, Kluwer Academic Publishers, Boston
3 Chen, J., Brevet, A., Formant, M., Leveque, F., Schmitter, J.-M., Blanquet, S. and Plateau, P. (1990) Pyrophosphatase is essential for growth of *Escherichia coli*. J. Bacteriol. **172**, 5686–5689
4 Lundin, M., Baltscheffsky, H. and Ronne, H. (1991) Yeast *PPA2* gene encodes a mitochondrial inorganic pyrophosphatase that is essential for mitochondrial function. J. Biol. Chem. **266**, 12168–12172
5 Sonnewald, U. (1992) Expression of *E. coli* inorganic pyrophosphatase in transgenic plants alters photoassimilate partioning. Plant J. **2**, 571–581
6 Ogasawara, N. (2000) Systematic function analysis of *Bacillus subtilis* genes. Res. Microbiol. **151**, 129–134
7 Shintani, T., Uchiumi, T., Yonezawa, T., Salminen, A., Baykov, A. A., Lahti, R. and Hachimori, A. (1998) Cloning and expression of a unique inorganic pyrophosphatase from *Bacillus subtilis*: evidence for a new family of soluble inorganic pyrophosphatases. FEBS Lett. **439**, 263–266
8 Young, T. W., Kuhn, N. J., Wadeson, A., Ward, S., Burges, D. and Cooke, G. D. (1998) *Bacillus subtilis* ORF *yybQ* encodes a manganese-dependent inorganic pyrophosphatase with distinctive properties: the first of a new class of soluble pyrophosphatase? Microbiology **144**, 2563–2571
9 Cooperman, B. S., Baykov, A. A. and Lahti, R. (1992) Evolutionary conservation of the active site of soluble inorganic pyrophosphatase. Trends Biochem. Sci. **17**, 262–266
10 Baykov, A. A., Cooperman, B. S., Goldman, A. and Lahti, R. (1999) Cytoplasmic inorganic pyrophosphatases. Prog. Mol. Subcell. Biol. **23**, 127–150
11 Aravind, L. and Koonin, E. V. (1998) A novel family of predicted phoshoesterases includes *Drosophila* prune protein and bacterial RecJ exonuclease. Trends Biochem. Sci. **23**, 17–19
12 Merckel, M. C., Fabrichniy, I. P., Salminen, A., Kalkkinen, N., Baykov, A. A., Lahti, R. and Goldman, A. (2001) Crystal structure of *Streptococcus mutans* pyrophosphatase: a new fold for an old mechanism. Structure **9**, 289–297
13 Ahn, S., Milner, A. J., Fütterer, K., Konopka, M., Ilias, M., Young, T. W. and White, S. A. (2001) The "open" and "closed" structures of the type-C inorganic pyrophosphatases from *Bacillus subtilis* and *Streptococcus gordonii*. J. Mol. Biol. **313**, 797–811
14 Parfenyev, A. N., Salminen, A., Halonen, P., Hachimori, A., Baykov, A. A. and Lahti, R. (2001) Quaternary structure and metal-ion requirement of family II pyrophosphatases from *Bacillus subtilis*, *Streptococcus gordonii* and *Streptococcus mutans*. J. Biol. Chem. **276**, 24511–24518
15 Bateman, A. (1997) The structure of a domain common to archaebacteria and the homocystinuria disease protein. Trends Biochem. Sci. **22**, 12–13
16 Scott, J. W., Hawley, S. A., Green, K. A., Anis, M., Stewart, G., Scullion, G. A., Norman, D. G. and Hardie, D. G. (2004) CBS domains form energy-sensing modules whose binding of adenosine ligands is disrupted by disease mutations. J. Clin. Invest. **113**, 274–284
17 Ignoul, S. and Eggermont, J. (2005) CBS domains: structure, function, and pathology in human proteins. Am. J. Physiol. Cell Physiol. **289**, C1369–C1378
18 Kemp, B. E. (2004) Bateman domains and adenosine derivatives form a binding contract. J. Clin. Invest. **113**, 182–184
19 Niemeyer, M. I., Yusef, Y. R., Cornejo, I., Flores, C. A., Sepúlveda, F. V. and Cid, L. P. (2004) Functional evaluation of human ClC-2 chloride channel mutations associated with idiopathic generalized epilepsies. Physiol. Genomics **19**, 74–83
20 Bennetts, B., Rychkov, G. Y., Ng, H.-L., Morton, C. J., Stapleton, D., Parker, M. W. and Cromer, B. A. (2005) Cytoplasmic ATP-sensing domains regulate gating of skeletal muscle ClC-1 chloride channels. J. Biol. Chem. **280**, 32452–32458

Received 27 July 2007/20 August 2007; accepted 23 August 2007
Published as BJ Immediate Publication 23 August 2007, doi:10.1042/BJ20071017

21 Wellhauser, L., Kuo, H.-H., Stratford, F. L. L., Ramjeesingh, M., Huan, L.-J., Luong, W., Li, C., Deber, C. M. and Bear, C. E. (2006) Nucleotides bind to the C-terminus of ClC-5. Biochem. J. **398**, 289–294
22 Drake, H. L. and Daniel, S. L. (2004) Physiology of the thermophilic acetogen *Moorella thermoacetica*. Res. Microbiol. **155**, 869–883
23 Sambrook, J. and Russel, D. W. (2001) Molecular Cloning: A Laboratory Manual, 3rd edn, Cold Spring Harbor Laboratory Press, Cold Spring Harbor
24 Gasteiger, E., Hoogland, C., Gattiker, A., Duvaud, S., Wilkins, M. R., Appel, R. D. and Bairoch, A. (2005) Protein identification and analysis tools on the ExPASy server. In The Proteomics Protocols Handbook (Walker, J. M., ed.), pp. 571–607, Humana Press, Totowa
25 Baykov, A. A. and Avaeva, S. M. (1981) A simple and sensitive apparatus for continuous monitoring of orthophosphate in the presence of acid-labile compounds. Anal. Biochem. **116**, 1–4
26 Chervenka, C. H. (1972) Methods for the Analytical Ultracentrifuge, pp. 23–33, Spinco Division of Beckman Instruments, Palo Alto
27 Baykov, A. A., Dudarenkov, V. Y., Käpylä, J., Salminen, T., Hyytiä, T., Kasho, V. N., Husgafvel, S., Cooperman, B. S., Goldman, A. and Lahti, R. (1995) Dissociation of hexameric *Escherichia coli* inorganic pyrophosphatase into trimers on $His^{136} \rightarrow Gln$ or $His^{140} \rightarrow Gln$ substitution and its effect on enzyme catalytic properties. J. Biol. Chem. **270**, 30804–30812
28 Kuhn, N. J., Wadeson, A., Ward, S. and Young, T. W. (2000) *Methanococcus jannaschii* ORF mj0608 codes for a class C inorganic pyrophosphatase protected by Co^{2+} or Mn^{2+} ions against fluoride inhibition. Arch. Biochem. Biophys. **379**, 292–298
29 Meyer, S., Savaresi, S., Forster, I. C. and Dutzler, R. (2007) Nucleotide recognition by the cytoplasmic domain of the human chloride transporter ClC-5. Nat. Struct. Mol. Biol. **14**, 60–66
30 Zyryanov, A. B., Vener, A. V., Salminen, A., Goldman, A., Lahti, R. and Baykov, A. A. (2004) Rates of elementary catalytic steps for different metal forms of the family II pyrophosphatase from *Streptococcus gordonii*. Biochemistry **43**, 1065–1074
31 Kery, V., Poneleit, L. and Kraus, J. P. (1998) Trypsin cleavage of cystathionine-β-synthase into an evolutionarily conserved active core: structural and functional consequences. Arch. Biochem. Biophys. **355**, 222–232
32 Jhee, K. H., McPhie, P. and Miles, E. W. (2000) Domain architecture of the heme-independent yeast cystathionine-β-synthase provides insights into mechanisms of catalysis and regulation. Biochemistry **39**, 10548–10556
33 Carr, G., Simmons, N. and Sayer, J. (2003) A role for CBS domain 2 in trafficking of chloride channel CLC-5. Biochem. Biophys. Res. Commun. **310**, 600–605
34 Bieman-Oldehinkel, E., Mahmood, N. B. N. and Poolman, B. (2006) A sensor for intracellular ionic strength. Proc. Natl. Acad. Sci. U.S.A. **103**, 10624–10629
35 Zyryanov, A. B., Shestakov, A. S., Lahti, R. and Baykov, A. A. (2002) Mechanism by which metal cofactors control substrate specificity in pyrophosphatase. Biochem. J. **367**, 901–906
36 Zhang, R., Evans, G., Rotella, F. J., Westbrook, E. M., Beno, D., Huberman, E., Joachimiak, A. and Collart, F. R. (1999) Characteristics and crystal structure of bacterial inosine-5′-monophosphate dehydrogenase. Biochemistry **38**, 4691–4700
37 Miller, M. D., Schwarzenbacher, R., von Delft, F., Abdubek, P., Ambing, E., Biorac, T., Brinen, L. S., Canaves, J. M., Cambell, J., Chiu, H. J. et al. (2004) Crystal structure of a tandem cystathionine-β-synthase (CBS) domain protein (TM0935) from *Thermotoga maritima* at 1.87 Å resolution. Proteins **57**, 213–217
38 Dutzler, R. and Meyer, S. (2006) Crystal structure of the cytoplasmic domain of the chloride channel ClC-0. Structure **14**, 299–307
39 Phillips, R. (1966) Adenosine and the adenine nucleotides: ionization, metal complex formation and conformation in solution. Chem. Rev. **66**, 501–527
40 Bateman, A., Coin, L., Durbin, R., Finn, R. D., Hollich, V., Griffiths-Jones, S., Khanna, A., Marshall, M., Moxon, S., Sonnhammer, E. L. et al. (2004) The Pfam protein families database. Nucleic Acids Res. **32**, D138–D141
41 Heinonen, J. and Drake, H. L. (1988) Comparative assessment of inorganic pyrophosphate and pyrophosphatase levels in *Escherichia coli*, *Clostridium pasterianum* and *Clostridium thermoaceticum*. FEMS Microbiol. Lett. **52**, 205–208
42 Lundie, L. L. and Drake, H. L. (1984) Development of a minimally defined medium for the acetogen *Clostridium thermoaceticum*. J. Bacteriol. **159**, 700–703